Lab on a Chip

PAPER

View Article Online
View Journal | View Issue

Cite this: *Lab Chip*, 2021, **21**, 1811

A thermoelectrically stabilized aluminium acoustic trap combined with attenuated total reflection infrared spectroscopy for detection of *Escherichia coli* in water

Stephan Freitag, [a] Bettina Baumgartner, [a] Stefan Radel,[a] Andreas Schwaighofer, [a] Antonio Varriale,[b] Angela Pennacchio,[b] Sabato D'Auria [b] and Bernhard Lendl *[a]

Received 11th December 2020,
Accepted 10th March 2021

DOI: 10.1039/d0lc01264e

rsc.li/loc

Acoustic trapping is a non-contact particle manipulation method that holds great potential for performing automated assays. We demonstrate an aluminium acoustic trap in combination with attenuated total reflection Fourier-transform infrared spectroscopy (ATR-FTIR) for detection of *E. coli* in water. The thermal conductivity of aluminium was exploited to thermo-electrically heat and hold the acoustic trap at the desired assay temperature of 37 °C. Systematic characterisation and optimisation of the acoustic trap allowed high flow rates while maintaining high acoustic trapping performance. The ATR element serves not only as a reflector for ultrasound standing wave generation but also as a sensing interface. The enzyme conversion induced by alkaline phosphatase-labelled bacteria was directly monitored in the acoustic trap using ATR-FTIR spectroscopy. Sequential injection analysis allowed automated liquid handling, including non-contact bacteria retention, washing and enzyme-substrate exchange within the acoustic trap. The presented method was able to detect *E. coli* concentrations as low as 1.95 × 10^6 bacteria per mL in 197 min. The demonstrated ultrasound assisted assay paves the way to fully automated bacteria detection devices based on acoustic trapping combined with ATR-FTIR spectroscopy.

Introduction

Safe drinking water is essential to health and is a basic human right.[1] *Escherichia coli (E. coli)* is used as an indicator organism for faecal pollution in assessing drinking water quality.[2] The gold standard for detection of *E. coli* in water is membrane filtration followed by incubation and plate counting.[3] However, the colony counting required for this classic cultivation-based approach is labour and time intensive (18–24 h). Automated detection schemes for microbial pollution that speed up water monitoring are thus demanded by public authorities and water suppliers.[4] This need has been targeted by a variety of non-cultivation-based methods. Detection schemes based on quantitative polymerase chain reaction (qPCR), enzymatic methods and enzyme-linked immunosorbent assays (ELISA) exist and are in use for several years to assess water-based public health risks.[5–7] Techniques based on immunomagnetic separation have also been employed for the quantification of *E. coli* in water.[8] Paper-based and microfluidic assay approaches are also emerging as cost-effective alternatives.[9,10]

Ultrasound (US) particle manipulation has shown great potential in the life sciences and bioanalytical chemistry, as it is label-free, non-invasive and easily implemented.[11,12] It has been employed for handling of particles,[13,14] cells[15,16] and bacteria.[17–21] Particle manipulation is achieved *via* an ultrasound standing wave (USW) generated between a piezoelectric transducer—operated at frequencies around 2 or 4 MHz—and a reflector *via* superposition of the incident and the reflected wave in the cavity between the US source and the reflector. The resulting acoustic radiation force[22] is used to guide particles in a process known as acoustophoresis[23] or to immobilize particles against a flow by acoustic trapping.[24] Glass and silicon are the materials most commonly used to build acoustofluidic devices, but aluminium has been recently employed due to its low cost and convenient acoustic properties, as it has an acoustic impedance similar to silicon or glass.[13,14]

Acoustic trapping has previously been used to perform non-contact bead-based assays as well as bacteria trapping

[a] *Research Division of Environmental Analytics, Process Analytics and Sensors, Institute of Chemical Technologies and Analytics, Technische Universität Wien, Getreidemarkt 9/164-UPA, 1060 Vienna, Austria.*
E-mail: bernhard.lendl@twien.ac.at
[b] *Institute of Food Science, CNR, Via Roma 64, 83100 Avellino, Italy*

using seed particles.[25–28] US particle manipulation has been paired with near infrared,[29] attenuated total reflection Fourier-transform mid-infrared (ATR-FTIR) spectroscopy[30,31] and Raman spectroscopy[32] to enhance process analytical spectroscopy as well as with fluorescence and surface-enhanced Raman spectroscopy.[33] Mid-IR spectroscopy allows rapid, non-destructive, and label-free acquisition of molecule-specific information by probing molecular vibrations. Recent research introduced an acoustic trap for bead injection combined with ATR-IR spectroscopy,[34] which has been used in a wide variety of applications due to its robustness.[32,33] Here, total reflection of the IR light within the ATR element generates an evanescent field that penetrates the sample on top of the ATR element to a depth of up to 2 μm.[35]

In the present work, we exploited the thermal conductivity of aluminium to build a thermoelectrically (TE) stabilized acoustic trap. We combined the acoustic trap with a custom-made multi-bounce ATR-FTIR setup, where the ATR element not only acts as the sensing interface for IR spectroscopy but also as a reflector for USW generation, enabling real-time monitoring in the acoustic trap. Thorough characterization and optimization of the method's bacteria-trapping performance resulted in straightforward US-assisted bacteria handling. We were able to trap bacteria at flow rates up to 1.17 μL s^{-1}, which corresponds to an average fluid velocity in the acoustic trap *i.e.*, flow rate/cross section of 0.295 mm s^{-1} at the widest point. To demonstrate possible implementations of the developed device, we utilized the acoustic trap in an assay for bacteria monitoring. Optical read out in the proposed sensing scheme is performed by ATR-IR spectroscopy. The developed US-assisted assay was employed to quantify *E. coli* in water samples; concentrations down to 1.95×10^6 bacteria per mL could be observed. Herein, we demonstrate the feasibility of a cost-effective TE-stabilized aluminium acoustic trap combined with ATR-FTIR spectroscopy for bacteria analysis in water.

Experimental

Reagents and materials

Biotinylated polyclonal rabbit anti-*E. coli* antibody (ab68451) and alkaline phosphatase (AP) conjugated streptavidin (ab136224) was sourced from Abcam (Cambridge, United Kingdom). Polyoxyethylene (20) sorbitan monolaurate (Tween 20), diethanolamine (DEA), bovine serum albumin (BSA), sodium azide and Tris buffered saline (TBS) pH 7.6 tablets were purchased from Sigma-Aldrich (Steinheim, Germany); *p*-nitrophenylphosphate (*p*NPP) disodium hexahydrate was obtained from Boehringer-Mannheim (Mannheim, Germany); magnesium sulphate heptahydrate ($MgSO_4 \cdot 7H_2O$) and zinc sulphate heptahydrate ($ZnSO_4 \cdot 7H_2O$) were sourced from Merck (Darmstadt, Germany). Ethanol (absolute) was supplied by Chemlab (Zedelgem, Belgium). TBS was prepared by dissolving one TBS tablet in 500 mL deionized water. TBS-T was mixed by adding 0.1%$_{vol}$ Tween 20 to TBS. Antibody and streptavidin dilution buffer was produced by dissolving 1% (w/v) BSA and 0.02% (w/v) sodium azide in TBS. An enzyme substrate solution was prepared by dissolving 50 mmol L^{-1} *p*NPP in a 500 mmol L^{-1} DEA buffer containing 0.1 mmol L^{-1} Zn^{2+} and 1 mmol L^{-1} Mg^{2+}. The pH of the substrate solution was adjusted to 9.8 using hydrochloric acid, and 500 μL aliquots of the enzyme substrate were stored at −20 °C until use. The antibody was diluted to 20 μg mL^{-1} and streptavidin was diluted 1000-fold immediately before usage in the antibody dilution buffer.

E. coli growth and water sample preparation

A small amount of *E. coli* (strain RB792) from the laboratory strain collection was used to inoculate a Luria-Bertani (LB) agar plate. The agar plate was incubated at 37 °C for 16 h. Chosen colonies, grown on the solid medium, were used to inoculate 10 mL of liquid LB medium in a sterile 50 mL tube. The bacterial culture was incubated at 37 °C overnight, under orbital shaking (160 rpm). Following incubation, the cells were harvested by centrifugation, and the resulting pellet was washed three times with sterile distilled water. The *E. coli* suspension was then diluted to the final working concentration using distilled water.

The number of colony-forming units (CFU) of *E. coli* in each water sample was estimated *via* plate counting, where every colony represents a single bacterium present in the water sample. 20 μL of the sample were pipetted on a 90 mm plate count agar plate (VWR, Pennsylvania, United States) and incubated overnight at 37 °C. The sample was diluted such that each plate supported between 30 and 300 colonies. Three aliquots of every sample were incubated. The concentration of colony-forming *E. coli* in the sample was determined by multiplying the number of colonies found on the plate by the dilution factor. In addition, the overall amount of *E. coli* including colony-forming and non-colony-forming (dead) bacteria was determined by manual counting in a Thoma chamber.

Setup for ATR-FTIR spectroscopy

The experimental setup includes an acoustic trap on top of a multi-bounce ATR setup, linked to a US driver and a sequential injection analysis (SIA) system (Fig. 1).

The beam of a Vertex 70v (Bruker Optics, Ettlingen, Germany) FTIR spectrometer was guided through a custom-built ATR setup. The ATR fixture was 3D-printed using a Prusa

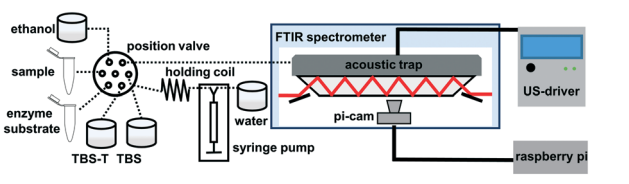

Fig. 1 Schematic of the acoustic trap on top of the ATR setup embedded into the FTIR spectrometer and linked to the ultrasound driver and the sequential injection analysis system with the pi-cam underneath.

Research i3 MK3 (Prague, Czech Republic) following blueprints constructed using Autodesk Inventor 2017 (Mill Valley, California, United States).[36,37] The multi-bounce zinc sulphide (ZnS) ATR element (17 × 10 × 1 mm, 45°) was sourced from Crystran (Poole, United Kingdom). The flow cell geometry allowed for five accessible total reflections. The calculated effective thickness (d_e) achieved with the ATR element is 17.25 μm.[35] After assembling the ATR setup, the acoustic trap was placed on top of the ATR element and sealed with an O-ring. The TE control was set to 37 °C throughout all assay experiments. Prior to spectrum acquisition, the spectrometer was evacuated and the sample compartment was flushed with dry air. A spectral resolution of 4 cm^{-1} was set for recording spectra in double-sided acquisition mode. Each spectrum was an average of 128 scans (acquisition time: 16.9 s), calculated using a three-term Blackman–Harris apodization function and a zero-filling factor of 2. The aperture was set to 8 mm for maximum intensity throughput. The FTIR spectrometer was equipped with a liquid-nitrogen-cooled mercury cadmium telluride (HgCdTe) detector. Spectra were analysed using the software package OPUS 8.2 (Bruker Optics, Ettlingen, Germany). The noise level of the setup was evaluated *via* 100% lines of the water-filled cell with turned-on US, yielding a root mean square noise of 1.02 × 10^{-5} AU between 1200 cm^{-1} and 1300 cm^{-1}.

The acoustic trap

Fig. 2 presents a scheme of the acoustic trap as well as a 3D model of the TE stabilized acoustic trap.

The acoustic trap was milled out of aluminium by Protolabs (Feldkirchen, Germany) following in-house-designed blueprints. The sample compartment has a volume of approximately 20 μL and a height of 500 μm. The cavity for US particle manipulation was formed by the 1 mm-thick ATR element, which worked as reflector, together with the piezo disc, which was glued to the aluminium body with a two-component epoxy resin (Polytec PT, Karlsbad, Germany). The dimensions of the aluminium layer between the piezo disc and liquid channel (see Fig. 2) were designed to optimize the energy density in the liquid layer, which is the guiding parameter for the radiation force exerted on suspended particles.[38] Based on an analytical solution for similar layered resonators, *i.e.* when the material properties change in only one direction, a 1.1 mm-thick aluminium layer was used between the liquid channel and the piezo transducer. The necessary calculations were performed in a self-written script in LabView based on the method from Nowotny and Benes.[39] In this approach, all physical properties, *e.g.* electrical admittance response and sound variables depending on the used materials and dimensions, are taken into account simultaneously. An 8 mm piezo disc (lead zirconium titanate, Type 181; PI Ceramics, Lederhose, Germany) with wrap-around silver electrodes was glued to the aluminium body. For thermal management, a Peltier element (5.8 W, 2.5 A, 3.8 V, 15 × 15 mm × 4.3 mm, RS Components, Corby United Kingdom) and a negative temperature thermistor (10 kΩ) were linked to a 1091 thermo-electrical controller (TEC; Meerstetter Engineering, Rubingen, Switzerland). The heatsink, mounted to the acoustic trap *via* nylon screws, was designed to have approximately the same thermal mass as the acoustic trap. A 30 × 30 mm 5 V fan was mounted to the sink. Throughout the experiments, the acoustic trap was thermally maintained at 37 °C. A sonicamp US signal generator (usePAT, Vienna, Austria) was connected to the piezo element *via* a coaxial cable. The optimal US operating frequency was determined *via* normalized differential impedance spectroscopy and the sinusoidal driving signal gain was set to 95% for all experiments, leading to a 26.6 V_{pp} US driving voltage. The heating induced by the high driving voltage could be easily countered by the TEC controller, allowing for stable bacteria trapping and unhampered FTIR spectroscopy.

Sample handling

Fig. 3 shows the liquid handling scheme of the SIA system.

The SIA system consisted of a 10-port selection valve from VICI (Schenkon, Switzerland) and a Carvo XC syringe pump from Tecan (Männerdorf, Switzerland) equipped with a 100 μL glass syringe. PTFE tubing (1/16 inch, inner diameter of 0.18 mm) from VICI (Schenkon, Switzerland) was used to connect the selection valve, the syringe pump and the solution containing vials, as well as for winding the holding coil. The ports of the selection valve were linked to the

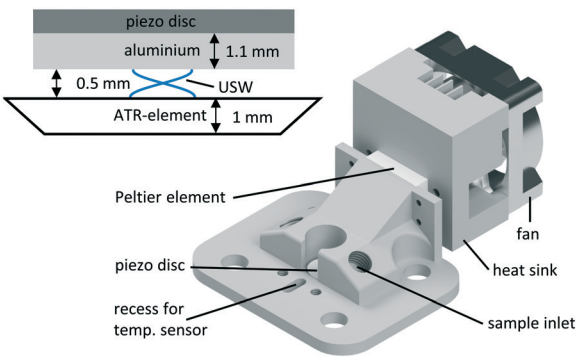

Fig. 2 Scheme and 3D model of the acoustic trap, including the Peltier element, heat sink and fan for thermo-electrical stabilization.

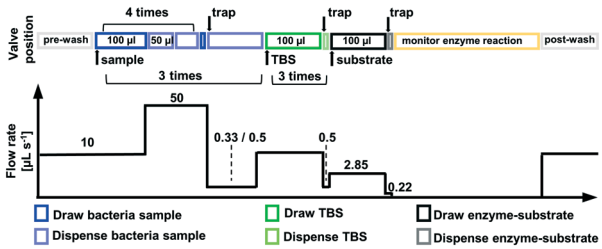

Fig. 3 Sequential injection sequence for fully automated handling of antibody-labelled *E. coli*, wash buffer and enzyme substrate.

sample vial, the enzyme substrate solution, TBS, TBS-T, the acoustic trap and the waste. The SIA setup and the software controlling the FTIR spectrometer were controlled *via* LabView (National Instruments, Austin, TX, USA) with a server–client program structure.[40]

Before the bacteria sample was put into the SIA system to perform the US-assisted assay, a procedure to label them with antibody was implemented. Therefore, a 1 mL aliquot of bacteria sample was pipetted into a 1.5 mL Eppendorf tube (Hamburg, Germany) and centrifuged for 5 min at 5000 rpm using an Eppendorf minispin centrifuge (Hamburg, Germany). After discarding the supernatant, the bacteria pellet was re-suspended in 500 μL of antibody solution and incubated for 60 min at room temperature and 10 rpm using a tube rotator (Thermo-Fisher Scientific, Darmstadt, Germany). The incubated bacteria suspension was again centrifuged for 5 min. Subsequently, the supernatant was discarded and the bacteria pellet was washed once with 1 mL TBS-T. Then the pellet was re-suspended in 500 μL of streptavidin solution and again incubated for 30 min on the tube rotator. In the end, two washing steps were performed using TBS-T and TBS. The bacteria sample was then resuspended in TBS, and 330 μL of the sample were pipetted into a fresh 1.5 mL tube, which was then placed in the SIA system. The next sample handling steps were fully automated *via* the SIA system according to the sequence depicted in Fig. 3. First, the acoustic trap was rinsed with 400 μL of TBS, then the bacteria sample was aspirated and withdrawn back into the sample vial four times to ensure homogenisation of the sample. Then, 300 μL of the bacteria sample where aspirated and injected into the acoustic trap; the first 100 μL were injected at 0.33 μL s^{-1}, and the following 200 μL were injected at 0.5 μL s^{-1}. Subsequently, 300 μL TBS was pumped through the acoustic trap to remove unbound antibody or streptavidin. Finally, 100 μL of enzyme substrate was injected into the acoustic trap. Directly after completion of the substrate injection, 30 consecutive IR spectra were recorded at 1 minute intervals. After monitoring the enzymatic reaction the acoustic trap was rinsed with water and 600 μL TBS-T, then with 200 μL of distilled water. To remove any air bubbles that may have been introduced, 100 μL of ethanol was injected, followed by 600 μL of distilled water. The US was active during the entire SIA sample handling and washing sequence. The flow rate was decreased while changing from TBS to substrate to counter shifts in the optimal working frequency *via* altered acoustic properties (Fig. 3).

Impedance spectroscopy

Electrical impedance spectra acquisition was done using a Sciospec ISX-3 (Bennewitz, Germany) electrical impedance spectrometer. The piezo disc on top of the acoustic trap was connected *via* the same coaxial cable to the external port adapter of the spectrometer that was later used to connect to the US driver. Spectra were recorded between 1 and 4 MHz using a resolution of 1.5 kHz (2000 steps), resulting in a measurement time of 790.19 ms per spectrum.

Camera system and image processing

A camera system was assembled to observe the acoustic trap through the transparent ZnS ATR element using a Raspberry Pi 2 coupled to a Pi camera B rev. 2.0 module from the Raspberry Pi foundation (Cambridge, United Kingdom). A light-emitting diode (LED) was mounted next to the camera, creating ideal conditions to film through the ATR crystal in the sample compartment of the FTIR spectrometer. The ceiling of the liquid channel in the acoustic trap was painted black to enhance the contrast for imaging using an Edding 780 marker (Ahrensburg, Germany). A script was developed to record pictures whenever desired. Raw images (1920 × 1080 pixels) recorded with the pi cam were further processed in ImageJ.[41] Before retaining bacteria in the acoustic trap, a picture of the empty cell was recorded. The following image processing sequence was performed on every image used for acoustic trap characterization: first, the image of the empty cell was subtracted from the image of interest. Then, the contrast was enhanced and a median filter with a 4 pixel radius was applied, followed by making the picture binary. The image was calibrated to the width of the acoustic trap and finally, the area of the *E. coli* clusters, marked *via* a threshold, was determined.

Results and discussion

Characterization of the acoustic trap

We performed an in-depth characterization of the acoustic trap on top of the ATR setup to identify the optimal working conditions for handling *E. coli* and ideal assay conditions regarding flow and bacteria retention. Following the introduction of water and equilibration of the setup to approx. 27.5 °C, the temperature was monitored using the TEC system sensor without TE control. A US frequency of 2 MHz was chosen to measure the thermal response of the system to different US driving signal gains.

As shown in Fig. 4A, operation of the piezo disc leads to increasing temperature over time, with a larger change found

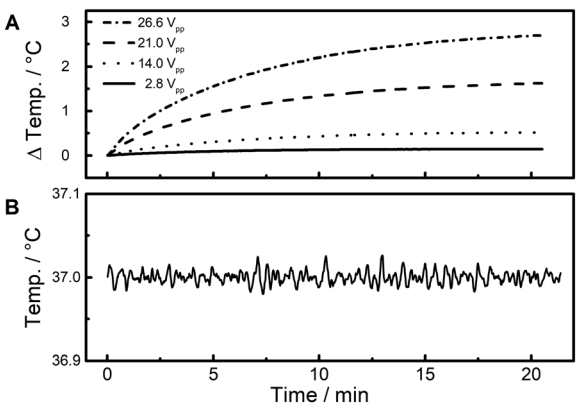

Fig. 4 A Heating induced by different piezo driving voltage for US generation measured *via* the TEC at an US frequency of 2 MHz. B Temperature stability of the acoustic trap reached *via* TE control at 95% (26.6 V_{pp}) driving signal.

for greater driving voltages applied *via* the US driver. Driving signals below 14 V_{pp} merely led to a temperature change, which could be countered by extending the equilibration time before starting the injection sequence (see Fig. 5A). For higher piezo driving voltages, active temperature control was necessary to provide stable conditions throughout the measurement run. For the final operating settings of the trap at 37 °C and 26.6 V_{pp} piezo driving voltage, we found a standard deviation during temperature stabilization of 7 mK, ensuring optimal assay conditions (Fig. 4B). These settings were applied for all experiments performed in this work. Further, we found that the liquids employed in the assay stored at room temperature passing through an aluminium inlet, as part of the TE controlled trap, did not affect the thermal stability of the system.

Typically, characterization of US devices for particle manipulation includes manual frequency tuning. Such trials are often accompanied by simultaneous observations of a particle suspension, *e.g. via* microscopy or the bare eye. These methods are cumbersome and highly user dependent, and hence subjective. Several more systematic approaches based on investigations of the electric response of the piezo transducer to altering currents have been proposed. Admittance/impedance,[15,27,42–44] and conductance[45] measurements can be used to better understand US particle manipulation devices, even allowing for feedback control.[27] However, the data obtained with those methods is still not easy to interpret as resonances are not only linked to the liquid channel.[43,44] Recently, Vitali *et al.* reported an approach based on differential impedance spectra analysis to find the optimal working frequency.[46] In this straightforward method, the resonance frequency linked to the liquid channel is identified by altering the acoustic properties of the liquid, hence changing the resonance condition of the channel. We applied this method to our device by connecting a commercially available electrical impedance spectrometer and performing impedance measurements of the trap filled with different solutions. To achieve this, the trap was mounted on top of the ATR-IR setup and filled with water. The temperature was set to 37 °C. After recording the impedance spectrum of pure water, the acoustic trap was filled with a $1\%_{vol}$ ethanol in water solution to alter the acoustic properties of the liquid channel, and an impedance spectrum was again recorded (Fig. 5A). From the measured data, the complex-valued impedance was calculated for the water-filled trap and the ethanol solution using the following equation:

$$\hat{Z} = |\hat{Z}| \exp\left(\frac{i\phi\pi}{180°}\right) \quad (1)$$

where $\hat{Z}$ is the complex valued impedance, $|\hat{Z}|$ is the impedance magnitude and φ is the phase angle.

The normalized differential impedance spectrum (NDS) was calculated *via*[46]

$$\mathrm{NDS} = \frac{\left|\hat{Z}_{\mathrm{water}} - \hat{Z}_{1\%\,\mathrm{ethanol}}\right|}{\left|\hat{Z}_{\mathrm{water}}\right|}. \quad (2)$$

The impedance magnitude spectrum of the acoustic trap containing water shows only small changes compared to the ethanol-solution-filled trap (Fig. 5A). The spectrum suggests an operation of the trap at the prominent impedance minimum at 2.08 MHz, linked to the resonant frequency of the piezo disc, where the transfer of electrical energy into mechanical energy

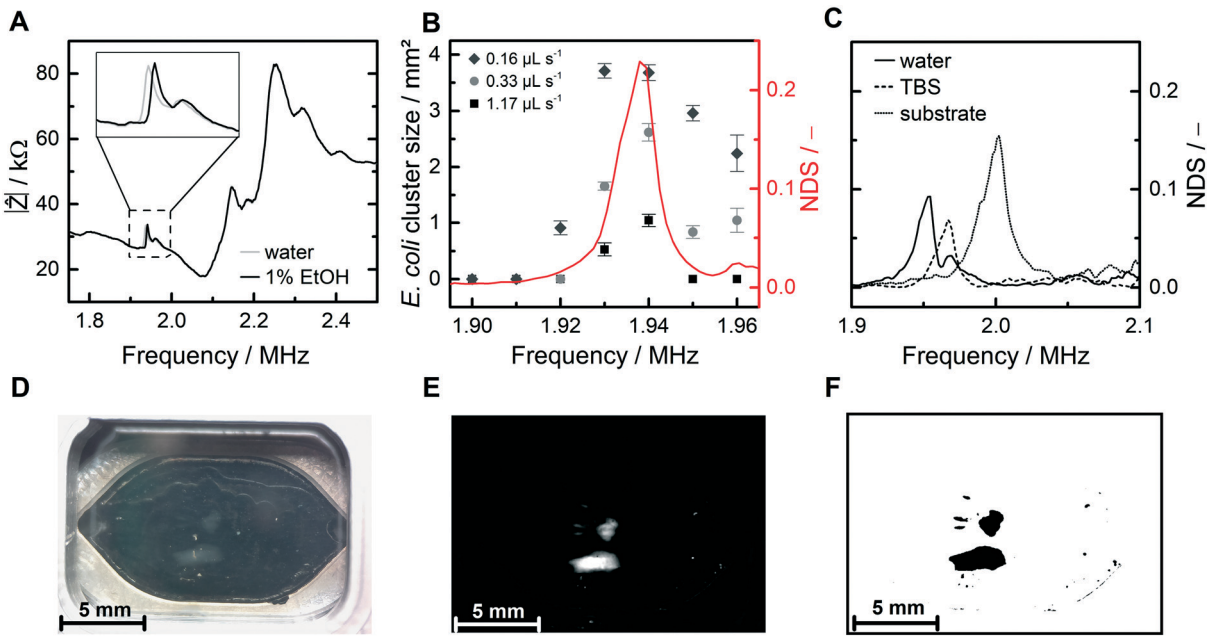

Fig. 5 A Impedance magnitude spectra of the acoustic trap filled with water and ethanol solution. B Results of the acoustic trap characterization *via* image processing guided by normalized differential impedance spectra (NDS, red line) for different trapping flows. C NDS after reassembly of the trap for water, TBS and enzyme substrate. D Picture of the acoustic trap showing *E. coli* clusters. E Differential picture after subtraction of the image of the empty acoustic trap. F Binary picture of *E. coli* clusters before measuring cluster size *via* a threshold.

is the most efficient. In contrast to the impedance magnitude spectra (Fig. 5A) with their detailed information content about the entire acoustic resonator, evaluation by NDS (Fig. 5B and C) offers an explicit and straightforward way to determine the resonance frequency of the liquid channel. The optimum working frequency of the water-filled trap was thus determined to be 1.94 MHz.

After initial NDS experiments, we evaluated the trapping capabilities of the device for a 100 μL *E. coli* sample containing 9.75×10^7 bacteria per mL pumped through the trap at different flow rates. The experiment was observed *via* the camera system. Immediately after sample injection by the SIA system, an image was recorded *via* the camera. At low flow and operation at the frequency suggested *via* NDS, *E. coli* cluster formation could be easily observed with the bare eye (Fig. 5D). Image processing (Fig. 5E and F) allowed determination of the size of the *E. coli* clusters at different parameters (Fig. 5B). Bacteria trapping experiments were performed at the optimum frequency calculated *via* NDS as well as at higher and lower frequencies in 10 kHz steps. Every trapping experiment was conducted three times. Results showed that the ideal operating frequency (1.94 MHz) of the trap with the highest acoustic energy density in the liquid layer was different than the eigenfrequency of the piezo element (2.08 MHz). Trapping of bacteria was possible at flow rates up to 1.17 μL s^{-1} when operating the cell at 1.94 and 1.93 MHz, which is in good accordance with the NDS. For lower flow rates, bacteria trapping is possible at a wider range of frequencies. Furthermore, the bacteria cluster size at the ideal operating frequency also increases with decreasing flow (Fig. 5B). Hence, for the assay the first 100 μL of bacteria sample was injected at 0.33 μL s^{-1}, followed by double injection at 0.5 μL s^{-1}.

Our findings demonstrate that the developed aluminium-based acoustic trap is capable to trapping *E. coli* at flow rates up to 1.17 μL s^{-1}. In addition, the presented results confirm previous reports that NDS is a strong tool for straight-forward identification of the optimal working frequency for an acoustofluidic device to optimize particle manipulation. We demonstrated that the use of aluminium for the acoustic trap material allows for elegant temperature control of the whole device, allowing counteraction of the heating induced by the piezo and enabling high driving voltages, which result in high acoustic energy densities in the liquid channel.[22]

After performing *E. coli* trapping experiments with the water-filled trap, the resonator was disassembled, thoroughly cleaned and reassembled. The same procedure to find the optimum working frequency *via* NDS was then performed again for water, TBS and enzyme substrate. In the assay, the bacteria were re-suspended in this buffer after isolation from water. It was found, that the ideal working frequency of the water filled cell shifted by 10 kHz after reassembly (compare Fig. 5B and C). An exact remount of the acoustic trap on top of the ATR fixture after disassembly is not possible, explaining this shift. Furthermore, the difference in the speed of sound between water, TBS and the DEA enzyme substrate buffer leads to a different optimum frequency for all three liquids. This further underlines the usefulness of NDS, as it could be used for fast characterisation of demountable acoustic resonators, where precise reproduction of the liquid layer is nearly impossible. Based on these findings the flow rate during liquid exchange from TBS to the enzyme substrate was reduced during the final assay (Fig. 3). As the bacteria were resuspended in TBS after isolation from water the operating frequency was set to 1.97 MHz throughout the entire assay sequence.

Ultrasound-assisted assay for *E. coli* in water using the acoustic trap

After determining the optimal working conditions of the acoustic trap, an US-assisted assay utilizing the acoustic trap for analysing water samples with different amounts of *E. coli* was performed. During this liquid handling sequence acoustically trapped *E. coli* cells serve as carrier for the enzyme alkaline phosphatase. Bacteria were isolated *via* centrifugation, incubated with a biotinylated antibody and AP conjugated to streptavidin. Then the antibody-labelled bacteria were re-suspended in TBS and injected into the system using the fully automated SIA sequence depicted in Fig. 3 and described in the liquid handling section. After completing the SIA sequence, IR spectra of the conversion of the enzyme substrate *p*NPP into the products *p*-nitrophenol and phosphate by AP-labelled *E. coli* were recorded over the course of 30 min with a time resolution of 1 min. IR difference spectra of the enzymatic reaction were calculated by[47]

$$\Delta A = \log\left(\frac{I_0}{I_{(t)}}\right) \quad (3)$$

where I_0 is the spectrum directly recorded after completed injection of the enzyme substrate and $I_{(t)}$ are the subsequent spectra recorded one minute apart.

The scheme of the chemical reaction is shown as inset in Fig. 6A (a detailed description is given in ref. 18). To summarize, the prominent band between 1250 and 1325 cm^{-1} is linked to the symmetric stretching vibration of the nitro group $\nu_s(NO_2)$. The enzymatic cleavage by AP of the phosphate moiety leads to a red shift of the NO_2 vibrational mode; thus, this band emerges as the enzymatic conversion proceeds. The band height was used as an analytical signal after baseline correction (Fig. 6A).

The thermal conductivity of the employed aluminium acoustic trap enabled optimal enzyme reaction conditions, as the desired temperature of 37 °C for AP could be easily maintained throughout the assay *via* TE stabilization.[48] It was found that the TBS washing step and the final injection of enzyme substrate did not hamper bacteria retention, as the flow rate was decreased while changing from TBS to enzyme substrate to counter shifts in the optimal working frequency *via* altered acoustic properties (Fig. 5C). Higher *E. coli* concentrations led to increasing enzymatic conversion rates observed directly in the trap *via* the characteristic IR bands of the enzymatic product. This allowed for

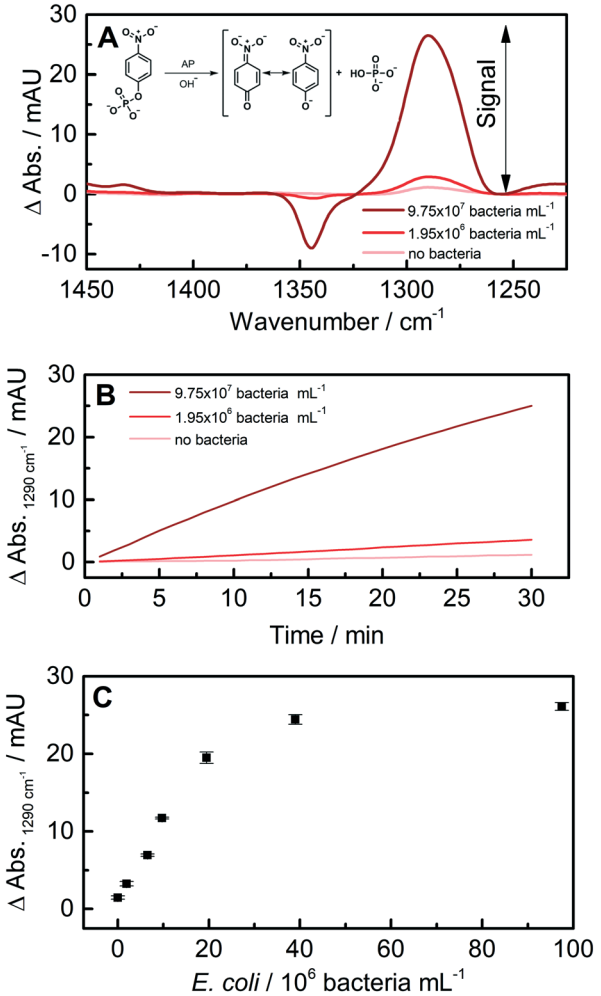

Fig. 6 A Reaction scheme and Δ absorbance after 30 min of enzyme conversion for different *E. coli* concentrations. B Real-time monitoring of the ongoing enzymatic reaction in the acoustic trap. C Analytical signal obtained after 30 min of enzyme conversion for different concentrations of *E. coli* in water samples.

quantification of different amounts of *E. coli* in water as low as 1.95×10^6 bacteria per mL. The linear range of the developed method was found to be between 1.95×10^6 and 1.95×10^7 bacteria per mL (Fig. 6C). Every experiment was conducted three times, showing excellent reproducibility, facilitated by the straightforward non-contact nature of acoustic trapping, paired with automated sample handling and washing *via* the SIA system.

Regarding the analysis time, the presented technique showed potential for high throughput application. The procedure consists of two parts. First, the bacteria handling scheme for isolation and incubation with antibodies and the AP-labelled streptavidin is 120 min, including all centrifugation and washing steps. This part can be potentially performed in batch or staggered for multiple samples. Second, the total sample handling and measurement time performed in the acoustic trap amounts to 77 min, including bacteria trapping, washing with TBS, injection of substrate, monitoring the reaction *via* ATR-IR spectroscopy (30 min), and the post- and pre-wash procedure. Consequently, the total analysis time of the first sample amounts to 197 min, while it is 77 min for every subsequent sample of the pre-treated batch.

Conclusions

Acoustic trapping holds great potential for performing non-contact assays involving different kinds of particles. Classic acoustic traps are mostly made of glass or silicon;[17,24,26] however, recent acoustofluidic devices based on aluminium have shown promising results for particle manipulation.[13,14,34] Thus, aluminium-based acoustic traps represent a low-cost alternative that can be easily manufactured in comparison to glassware. We took advantage of the thermal conductivity of aluminium to build a TE-controlled trap, which allowed us to perform our assay at the desired 37 °C and which further counteracted thermal drifts induced by the high gain of the piezo driving signal or environmental influences.

Enzyme conversion could be directly measured in the trap, with the ATR element serving as a sensing interface in addition to acting as the reflector for USW generation. We demonstrated that the developed acoustic trap is capable of retaining bacteria at a concentration of 1.95×10^6 bacteria per mL. A previous study demonstrated that the capability of an acoustic device to manipulate *E. coli* depends on the concentration of *E. coli* in suspension.[21] A more recent report on acoustic trapping of *E. coli* states a critical concentration of 5×10^7 bacteria per mL, at lower concentration bacteria trapping was not possible anymore, as acoustic streaming inhibited bacteria trapping.[17] The better performance of the presented aluminium acoustic trap might be linked to the geometry of the sample compartment. The height of the herein presented acoustic trap (0.5 mm) is larger than the half-wavelength resonance of the optimal working frequency of 1.94 MHz, which should yield a half-wavelength in water at 37 °C of approximately 0.390 mm. Together with the elliptic geometry of the acoustic trap this could suppress disruptive acoustic streaming patterns,[53] suggesting a numerical study of the developed device. In this context, an increased performance of US particle manipulation of bacteria by altering the acoustic streaming velocity field was previously described.[20] The presented setup allows for bacteria retention at higher flow rates compared to a previous study (0.16 μL s^{-1} *vs.* 1.17 μL s^{-1}).[17] This improvement can be explained by the geometry of the employed acoustic trap, as the demonstrated aluminium trap has a cross-section of 4 mm^2 (8 mm wide, 0.5 mm high). This results in an average fluid velocity *i.e.*, flow rate/cross section of 0.295 mm s^{-1} at the widest point of the acoustic trap. A narrower liquid channel would result in a higher average fluid velocity hence only allowing smaller flow rates.

We quantified the total number of bacteria by manual counting in a Thoma chamber and performed enumeration of living bacteria *via* CFU. We found that living and dead bacteria

can be trapped, as the concentration of 9.75×10^7 bacteria per mL used for acoustic trap characterization corresponds to 5.92×10^4 CFU mL^{-1}. Dead *E. coli* cells contribute to the bacteria trapping performance, as secondary acoustic radiation forces form between living and dead bacteria. This is underlined by the size of the cluster shown in Fig. 5D formed by 100 μL of 5.92×10^4 CFU mL^{-1} (9.75×10^7 bacteria per mL). If only living colony-forming cells would be acoustically trapped the cluster should have a size of 0.01 mm^2, assuming the size of a single *E. coli* to be 1×2 μm.[49]

As reported in a previous study, the retention and thus the detection of *E. coli* at lower concentrations is feasible with the use of bigger seed particles.[17] Further improvements in sample throughput *via* higher flow might be also facilitated by feedback control of the optimal working frequency of the liquid channel during liquid exchange to counter changing acoustic properties linked to different liquids pumped through the trap.[27] Hence, the proposed US-assisted assay could be also used at lower bacteria concentrations by employing seed particles.[17,21]

In a broader context, the presented US assisted assay for measuring *E. coli* in water cannot compete with other recently published methods such as surface plasmon resonance[50] or microfluidic fluorescent-based methods (5 CFU mL^{-1} at a total analysis time of 60 min)[10] in terms of limit of detection or analysis time. However, these methods rely on a sensitive surface or magnetic labels for manipulation, while our technique does not require labels for bacteria isolation or a sensitive surface. Moreover, those methods aim to measure colony-forming bacteria, whereas our method can also detect non-colony forming bacteria.

The excellent bacteria trapping capabilities of our device are connected to the achievable high driving voltages of the piezo enabled by TE stabilization, leading to greater acoustic energy density in the liquid channel,[22] paired with the systematic identification of the ideal working frequency *via* NDS. Acoustic trap characterization combining NDS and image processing suggests the combination of our trap with a more sophisticated imaging system (*e.g.* hyperspectral imaging). In addition, the recently reported possibility of performing antibody labelling with the assistance of ultrasound particle manipulation on a chip,[25] combined with on-chip mid-IR sensing[51,52] points to possibly automating the overall sample handling scheme, including antibody labelling, in addition to indicating room for further miniaturization. Mid-IR sensing in general holds the potential for label-free sensing by either directly measuring bacteria or their intrinsic β-D-galactosidase or β-D glucuronidase enzyme activity.[6] Here, TE stabilization of the acoustic trap enabled by using aluminium should also accelerate the transition of acoustofluidic devices from the lab into harsher environments. Together with the trend towards small handheld mid-IR spectrometers,[37] this addresses the need for completely automated water monitoring. Therefore, our future efforts will focus on developing ultrasound-assisted mid-IR sensing schemes in a completely label-free manner, beyond bacteria detection towards other cell types and catalytic particles.

Author contributions

Stephan Freitag: conceptualization, methodology, investigation, formal analysis, visualization, writing – original draft; Bettina Baumgartner: resources, writing – review & editing; Stefan Radel: methodology, writing – review & editing; Andreas Schwaighofer: supervision, visualization, writing – review & editing, Antonio Varriale: resources, writing – review & editing; Angela Pennacchio: resources; Sabato D'Auria: funding acquisition; Bernhard Lendl: conceptualization, supervision, writing – review & editing, funding acquisition.

Conflicts of interest

There are no conflicts to declare.

Acknowledgements

Martin Bulst of Sciospec is acknowledged for his help with impedance spectroscopy. This work received funding from the European Union's Horizon 2020 research and innovation programme through the project WaterSpy under grant agreement no. 731778 as well as from the COMET Center CHASE (project No 868615), which is funded within the framework of COMET (Competence Centers for Excellent Technologies) by BMVIT, BMDW, and the Federal Provinces of Upper Austria and Vienna. The COMET program is run by the Austrian Research Promotion Agency (FFG). The authors also acknowledge TU Wien Bibliothek for financial support through its Open Access Funding Program.

Notes and references

1 WHO, *Guidelines for drinking-water quality*, World Health Organization, Geneva, Switzerland, 2017.
2 S. Edberg, E. Rice, R. Karlin and M. Allen, *J. Appl. Microbiol.*, 2000, **88**, 1068–1168.
3 M. Grant, *Appl. Environ. Microbiol.*, 1997, **63**, 3526–3530.
4 N. Doulamis, A. Voulodimos, A. Doulamis, M. Bimpas, A. Angeli, N. Bakalos, A. Giusti, P. Philimis, A. Varriale and A. Ausili, *Sensors*, 2019, **19**, 33.
5 M. Botes, M. de Kwaadsteniet and T. E. Cloete, *Anal. Bioanal. Chem.*, 2013, **405**, 91–108.
6 K. Demeter, J.-B. Burnet, P. Stadler, A. Kirschner, M. Zessner and A. H. Farnleitner, *Curr. Opin. Environ. Sci. Health*, 2020, **16**, 82–91.
7 N. Wang, M. He and H.-C. Shi, *Anal. Chim. Acta*, 2007, **590**, 224–231.
8 G. Pappert, M. Rieger, R. Niessner and M. Seidel, *Microchim. Acta*, 2010, **168**, 1–8.
9 B. Pang, C. Zhao, L. Li, X. Song, K. Xu, J. Wang, Y. Liu, K. Fu, H. Bao and D. Song, *Anal. Biochem.*, 2018, **542**, 58–62.
10 Ü. Dogan, E. N. Kasap, F. Sucularlı, E. Yildirim, U. Tamer, D. Cetin, Z. Suludere, I. H. Boyaci and N. Ertas, *Anal. Methods*, 2020, **12**, 3788–3796.
11 A. Ozcelik, J. Rufo, F. Guo, Y. Gu, P. Li, J. Lata and T. J. Huang, *Nat. Methods*, 2018, **15**, 1021–1028.

12 P. Li and T. J. Huang, *Anal. Chem.*, 2018, **91**, 757–767.
13 G. P. Gautam, T. Burger, A. Wilcox, M. J. Cumbo, S. W. Graves and M. E. Piyasena, *Anal. Bioanal. Chem.*, 2018, **410**, 3385–3394.
14 W. N. Bodé, L. Jiang, T. Laurell and H. Bruus, *Micromachines*, 2020, **11**, 292.
15 J. P. Armstrong, S. A. Maynard, I. J. Pence, A. C. Franklin, B. W. Drinkwater and M. M. Stevens, *Lab Chip*, 2019, **19**, 562–573.
16 K. Xu, C. P. Clark, B. L. Poe, J. A. Lounsbury, J. Nilsson, T. Laurell and J. P. Landers, *Anal. Chem.*, 2019, **91**, 2186–2191.
17 B. Hammarström, T. Laurell and J. Nilsson, *Lab Chip*, 2012, **12**, 4296–4304.
18 S. Freitag, A. Schwaighofer, S. Radel and B. Lendl, *Proc. SPIE 10491*, San Francisco, 2018.
19 S. Gutiérrez-Ramos, M. Hoyos and J. Ruiz-Suárez, *Sci. Rep.*, 2018, **8**, 1–8.
20 M. Antfolk, P. B. Muller, P. Augustsson, H. Bruus and T. Laurell, *Lab Chip*, 2014, **14**, 2791–2799.
21 J. Hawkes, M. Limaye and W. Coakley, *J. Appl. Microbiol.*, 1997, **82**, 39–47.
22 H. Bruus, *Lab Chip*, 2012, **12**, 1014–1021.
23 F. Olm, H. C. Lim, K. Schallmoser, D. Strunk, T. Laurell and S. Scheding, *Cytometry, Part A*, 2020, DOI: 10.1002/cyto.a.24171.
24 M. Evander and J. Nilsson, *Lab Chip*, 2012, **12**, 4667–4676.
25 M. Binkley, M. Cui, M. Berezin and J. M. Meacham, *ACS Biomater. Sci. Eng.*, 2020, **6**, 6108–6116.
26 M. Tenje, H. Xia, M. Evander, B. Hammarström, A. Tojo, S. Belák, T. Laurell and N. LeBlanc, *Anal. Chim. Acta*, 2015, **853**, 682–688.
27 B. Hammarström, M. Evander, J. Wahlström and J. Nilsson, *Lab Chip*, 2014, **14**, 1005–1013.
28 B. r. Hammarström, B. Nilson, T. Laurell, J. Nilsson and S. Ekström, *Anal. Chem.*, 2014, **86**, 10560–10567.
29 T. Kambayashi, T. Noguchi, A. Nojima, S. Kono, S.-I. Taniguchi and Y. Ozaki, *Anal. Chem.*, 2020, **92**, 2946–2952.
30 C. Koch, M. Brandstetter, P. Wechselberger, B. Lorantfy, M. R. Plata, S. Radel, C. Herwig and B. Lendl, *Anal. Chem.*, 2015, **87**, 2314–2320.
31 N. Yamamoto, N. Kawashima, T. Kitazaki, K. Mori, H. Kang, A. Nishiyama, K. Wada and I. Ishimaru, *J. Biomed. Opt.*, 2018, **23**, 050503.
32 K. Wieland, S. Tauber, C. Gasser, L. A. Rettenbacher, L. Lux, S. Radel and B. Lendl, *Anal. Chem.*, 2019, **91**, 14231–14238.
33 N. Hao, Z. Pei, P. Liu, H. Bachman, T. D. Naquin, P. Zhang, J. Zhang, L. Shen, S. Yang and K. Yang, *Small*, 2020, 2005179.
34 S. Freitag, B. Baumgartner, S. Tauber, C. Gasser, S. Radel, A. Schwaighofer and B. Lendl, *Anal. Chem.*, 2019, **91**, 7672–7678.
35 G. Ramer and B. Lendl, in *Encyclopedia of Analytical Chemistry*, John Wiley & Sons, Ltd., Hoboken, New Jersey, USA, 2013.
36 B. Baumgartner, S. Freitag and B. Lendl, *Anal. Chem.*, 2020, **92**, 4736–4741.
37 B. Baumgartner, S. Freitag, C. Gasser and B. Lendl, *Sens. Actuators, B*, 2020, **310**, 127847.
38 J. J. Hawkes and S. Radel, *Lab Chip*, 2013, **13**, 610–627.
39 H. Nowotny and E. Benes, *J. Acoust. Soc. Am.*, 1987, **82**, 513–521.
40 C. Wagner, A. Genner, G. Ramer and B. Lendl, in *Modeling, Programming and Simulations Using LabVIEW Software*, InTech, Rijeka, Croatia, 2011.
41 M. D. Abràmoff, P. J. Magalhães and S. J. Ram, *Biophotonics Int.*, 2004, **11**, 36–42.
42 D. Carugo, T. Octon, W. Messaoudi, A. L. Fisher, M. Carboni, N. R. Harris, M. Hill and P. Glynne-Jones, *Lab Chip*, 2014, **14**, 3830–3842.
43 J. J. Hawkes, W. T. Coakley, M. Gröschl, E. Benes, S. Armstrong, P. J. Tasker and H. Nowotny, *J. Acoust. Soc. Am.*, 2002, **111**, 1259–1266.
44 J. Dual, P. Hahn, I. Leibacher, D. Möller and T. Schwarz, *Lab Chip*, 2012, **12**, 852–862.
45 D. M. Kalb, R. J. Olson, H. M. Sosik, T. A. Woods and S. W. Graves, *PLoS One*, 2018, **13**, e0207532.
46 V. Vitali, G. Core, F. Garofalo, T. Laurell and A. Lenshof, *Sci. Rep.*, 2019, **9**, 1–10.
47 W. Mäntele, *Trends Biochem. Sci.*, 1993, **18**, 197–202.
48 R. B. McComb, G. N. Bowers Jr and S. Posen, *Alkaline phosphatase*, Springer Science & Business Media, Berlin, Germany, 2013.
49 R. Phillips, J. Kondev, J. Theriot and H. Garcia, *Physical biology of the cell*, Garland Science, Taylor & Francis Group, New York, NY, USA, 2012.
50 Y. Li, J. Zhu, H. Zhang, W. Liu, J. Ge, J. Wu and P. Wang, *Sens. Actuators, B*, 2018, **259**, 492–497.
51 J. Haas, P. Artmann and B. Mizaikoff, *RSC Adv.*, 2019, **9**, 8594–8599.
52 N. T. Benéitez, B. Baumgartner, J. Missinne, S. Radosavljevic, D. Wacht, S. Hugger, P. Leszcz, B. Lendl and G. Roelkens, *Opt. Express*, 2020, **28**, 27013–27027.
53 P. B. Muller, R. Barnkob, M. J. H. Jensen and H. Bruus, *Lab Chip*, 2012, **12**(22), 4617–4627.